JOURNAL OF MATERIALS SCIENCE 29 (1994) 5693–5698

Oxidation protection of porous reaction-bonded silicon nitride

D. S. FOX
National Aeronautics and Space Administration, Lewis Research Center, Cleveland, OH 44135, USA

Oxidation kinetics of both as-fabricated and coated reaction-bonded silicon nitride (RBSN) were studied at 900 and 1000 °C with thermogravimetry. Uncoated RBSN exhibited internal oxidation and parabolic kinetics. An amorphous Si–C–O coating provided the greatest degree of protection to oxygen, with a small linear weight loss observed. Linear weight gains were measured on samples with an amorphous Si–N–C coating. Chemically vapour deposited (CVD) Si_3N_4 coated RBSN exhibited parabolic kinetics, and the coating cracked severely. A continuous–SiC–fibre–reinforced RBSN composite was also coated with the Si–C–O material, but no substantial oxidation protection was observed.

1. Introduction

Continuous–fibre–reinforced ceramic matrix composites are being investigated for possible application in advanced aerospace engines. This class of materials offers many benefits over conventional superalloys. The low weight, high temperature capability, excellent oxidation resistance and thermal shock resistance of these materials make them attractive. The major drawback of ceramics is their inherent brittle behaviour. Composite ceramics are being developed to overcome this problem. When cracks do form in the matrix, continuous fibres can deflect or bridge the cracks. Debonding of the fibre from the matrix also absorbs crack energy. Failure is therefore not catastrophic, as it would be in monolithic or particulate reinforced ceramics.

One such material that has been developed is a silicon carbide fibre (Textron SCS-6, Lowell, MA) reinforced reaction bonded silicon nitride (SiC–RBSN). The 142 μm diameter fibre has a carbon coating which provides the needed debonding mechanism for "graceful" failure. The processing of the composite has been previously described in detail [1]. The three-part process involves the use of polymer fugitive binders to create fibre mats and Si metal cloth, vacuum hot pressing of a sandwich of alternating layers of fibres and mats, and heat treatment in a nitrogen atmosphere to convert the silicon to silicon nitride. The resulting composite contains approximately 30 vol % fibres, and the matrix itself contains approximately 30 vol % porosity with an average pore size of 20 nm.

Dense, monolithic Si_3N_4 is highly oxidation resistant due to the formation of protective surface silica by the following reaction between solid, s, and gas, g

$$Si_3N_4(s) + 3O_2(g) = 3SiO_2(s) + 2N_2(g) \quad (1)$$

RBSN oxidizes via the same mechanism, though internal oxidation of the porous material comes into play. In the passive oxidation region

$$(\Delta W/A)^2 = k_p t \quad (2)$$

where $\Delta W/A$ is specific weight gain, and t is oxidation time. The parabolic rate constant, k_p, is determined via linear regression of the straight line formed when the kinetic data is plotted as the square of $\Delta W/A$ versus t.

An extensive review of all previous RBSN oxidation studies is outside the scope of this paper. Those dealing with oxidation kinetics are limited and reviewed here. At temperatures of 800–1000 °C, oxidation of internal porosity in RBSN dominates [2–7]. Weight gain, initially rapid, gradually slows with time. Since internal porosity remains open longer, overall weight gains are usually greater than those measured for the same material oxidized at higher temperatures [2–4, 6, 7].

At temperatures of 1200 °C and higher, porous RBSN has been found to exhibit a two-stage parabolic oxidation behaviour. When the kinetics are plotted as weight gain squared versus time, the data fall on two straight lines. At short times, the slope of the line is quite steep (k_p is large). This indicates that internal as well as external oxidation is occurring, with the former dominating. However, the pores quickly fill with SiO_2 and external oxidation governs, and the data sharply falls onto a line exhibiting a more gradual slope.

Some researchers have presumed that internal oxidation continues until the pore channels became completely blocked with silica [8, 9]. Porz and Thummler [7] determined that internal oxidation becomes negligible when open pores are sufficiently filled with SiO_2 that the mean pore channel radius becomes small enough to choke off further oxygen penetration into the pores. They found that a RBSN with open porosity < 10% and pore channels with mean radii of 20–30 nm exhibited good oxidation resistance. It

0022–2461

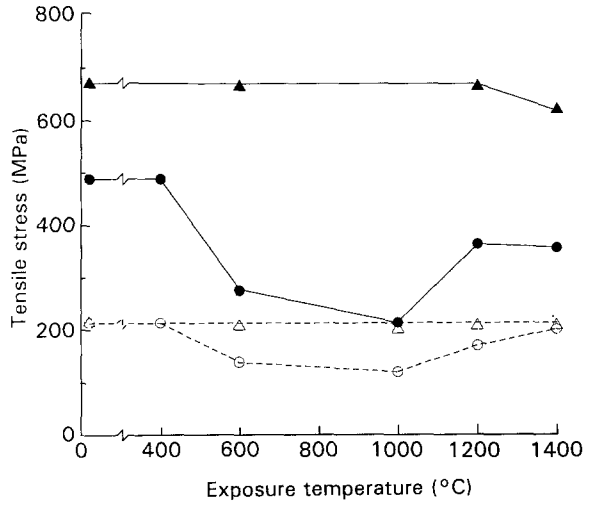

Figure 1 Room temperature tensile strength of SiC–RBSN after 100 h in flowing nitrogen (▲) or oxygen (●); First matrix room temperature cracking strength in (△) Nitrogen and (○) oxygen of same (adapted from Bhatt [3]).

should be noted that in the processing of SiC–RBSN, one has little control over the percentage and amount of open porosity in the RBSN matrix.

Oxidation of RBSN based composites is more complex than monolithic RBSN because of matrix porosity and microcracks, fibre coatings and interfaces, and exposed fibre ends. The oxidation of SiC–RBSN has been studied by Bhatt [3]. Fig. 1 summarizes the effect of 100 h exposures in two different atmospheres on tensile strength. Exposure in nitrogen to 1400 °C has little to no effect on either first matrix crack strength or the ultimate tensile strength of the composite (227 ± 40 MPa and 682 ± 150 MPa, respectively, at room temperature). However, tensile strength drops dramatically in the range 600–1000 °C after the material is heated in oxygen. This is due to gas transport through the porous matrix and the resulting oxidation of the carbon coating on the SiC fibres, as well as "tunnelling" of oxygen down the fibre core and interface from the unprotected ends of the composite. Behaviour improves at 1200 °C because the silica that grows on the surface of the composite adequately seals the matrix porosity and fibre ends, thereby minimizing oxidation of the carbon fibre coating. If this composite is to be used in a heat engine environment, it is obvious that a surface coating is needed to protect the material from oxidation.

As noted above, there is little control over percentage and amount of open porosity in the matrix due to processing constraints for SiC–RBSN. Coating systems are therefore the logical choice for oxidation protection. There has been some work to date in coating porous, monolithic reaction-bonded Si_3N_4 and SiC. Gregory and Richman [10] oxidized RBSN coated with 5 μm thick Si/5 μm thick Si_3N_4 at 1000 °C in ambient air. Weight gain was 55% that of uncoated RBSN after 100 h exposure. Adriaansen and Gooijer [11] coated RBSN having 20 vol % porosity with a 2 μm thick layer of chemically vapour deposited (CVD) Si_3N_4. Parabolic oxidation rate constants were 20–25% of that measured for uncoated RBSN at 1200 °C in flowing air. Desmaison *et al.* [12] also used CVD at 1275 °C to deposit a 6 μm thick layer of Si_3N_4 on RBSN containing 15–20 vol % porosity. Oxidation rate constants at 1100 °C in flowing oxygen were 300 times lower for the coated material. Other deposition temperatures and coating thicknesses provided a lesser degree of protection. Schlichting and Neumann [13] employed sol gel processing to coat reaction-bonded silicon carbide having 25 vol % porosity with SiO_2 and GeO_2–SiO_2 glasses. At 1000 °C in air the oxidation rate constants were 25 and 33%, respectively, of uncoated RBSC.

The purpose of the present paper is to investigate other coating systems for the oxidation protection of porous, monolithic reaction-bonded silicon nitride. Those coatings that act to substantially improve the oxidation resistance of the monolith are then used to coat a SiC–RBSN composite, and its oxidation behaviour is also reported.

2. Experimental procedure

Initial studies were conducted on uncoated, monolithic RBSN. Oxidation kinetics in dry flowing oxygen were followed with thermogravimetry at 900 and 1000 °C for up to 240 h. In addition, a number of coated coupons were also tested. Specimen size was approximately 2.5 × 1.0 × 0.2 cm. Uncoated samples were cleaned using detergent, distilled water, acetone and alcohol, and dried overnight at 100 °C. Those to be coated were delivered to each vendor. Type A samples were coated with a polymer precursor converted to an amorphous Si–N–C material (Ethyl Corporation, Baton Rouge, LA). Type B samples were impregnated with a polymer-derived, amorphous Si–C–O material (Allied Signal, Des Plaines, IL). A dense Si_3N_4 coating was grown on Type C samples (United Technologies, East Hartford, CT) via chemical vapour deposition (CVD).

Samples were suspended from a platinum chain in a vertical tube furnace having a quartz tube. Dry oxygen flowed from bottom to top. Weight changes were continuously monitored with a recording microbalance (Cahn 1000, Cerritos, CA). Ideally, in these types of experiments three samples should be run per condition. However, in the present study such numbers of specimens could not be supplied for testing. In all experiments using coated samples, just one sample was run. Surface morphologies before and after exposure were examined via scanning electron microscopy (SEM).

3. Results and discussion

3.1. Monolithic RBSN

Surface morphologies of the four types of samples are shown in Fig. 2. Characteristic porosity and 15 μm polishing scratches are observed on uncoated (Type U) RBSN. The Type A coating exhibited wide (1–3 μm) cracks and spallation at its topmost layer, and deeper layers were somewhat cracked, exposing the RBSN. The Type B coating did not have such a layered look. Cracks less than 1 μm wide were observed, but were not present to the extent noted in

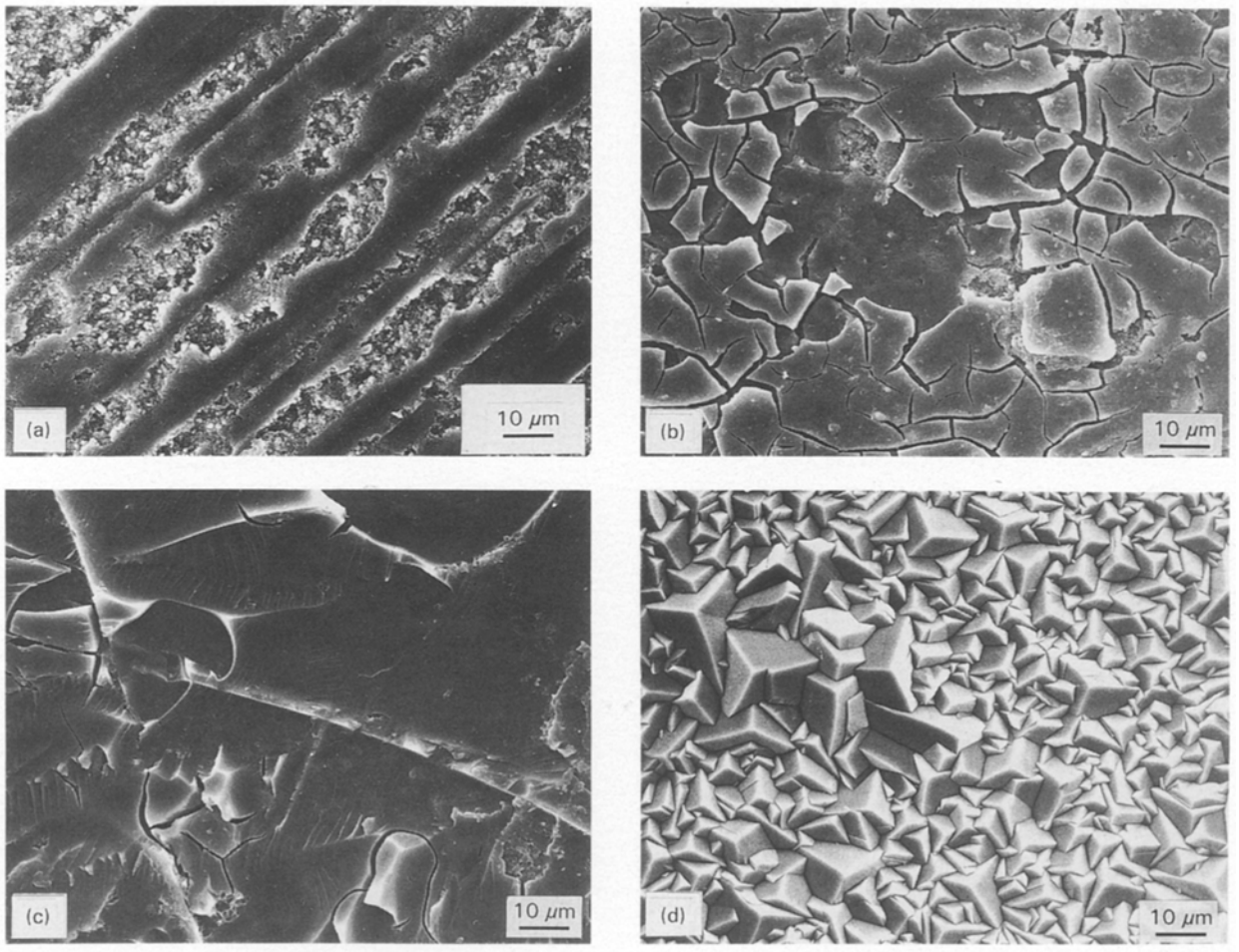

Figure 2 Surface morphology of monolithic RBSN prior to oxidation: (a) type U (uncoated), (b) type A (Si–N–C), (c) type B (Si–C–O), (d) type C CVD Si_3N_4.

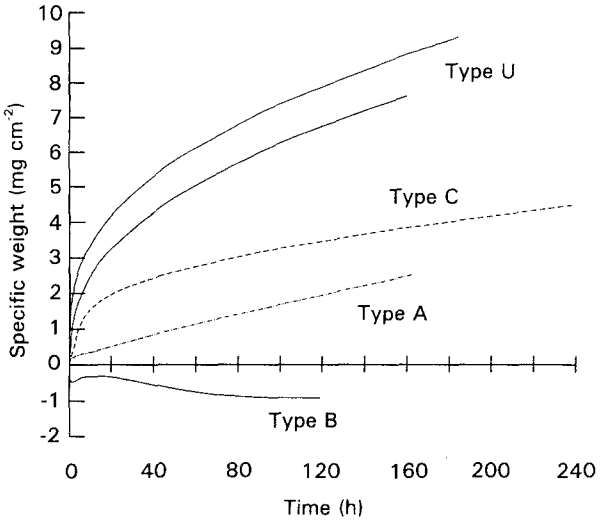

Figure 3 Oxidation kinetics of uncoated and coated monolithic RBSN at 900 °C in 100 cc min^{-1} dry flowing oxygen.

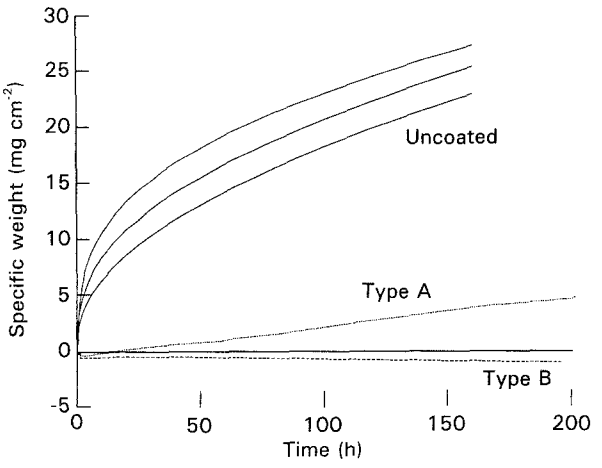

Figure 4 Oxidation kinetics of uncoated and coated monolithic RBSN at 1000 °C in 100 cc min^{-1} dry flowing oxygen.

Type A material. The CVD Si_3N_4 coating (Type C) had the characteristic faceted growth resulting from high temperature deposition. Porosity or cracking was not observed.

Kinetic results are shown in Figs 3 and 4, and surface morphologies after exposure in Fig. 5. The data is reported as weight gain per unit surface area of the sample. However, one must realize that the surface area of a porous RBSN sample 2.5 $\times$ 1.0 $\times$ 0.2 cm is much greater than the sum of the outer surface areas, or 6.4 cm^2. In this study, the kinetic curves for uncoated RBSN are therefore used as a reference for the coating systems investigated. Some previous papers have reported oxidation weight gains as $\Delta M/M_o$ (%) where M is mass. For this reason, the kinetic data from this investigation are also reported in such fashion in Table I.

Uncoated RBSN exhibited parabolic kinetics. Internal oxidation occurred, that slowed as the pores became more constricted due to silica formation, at

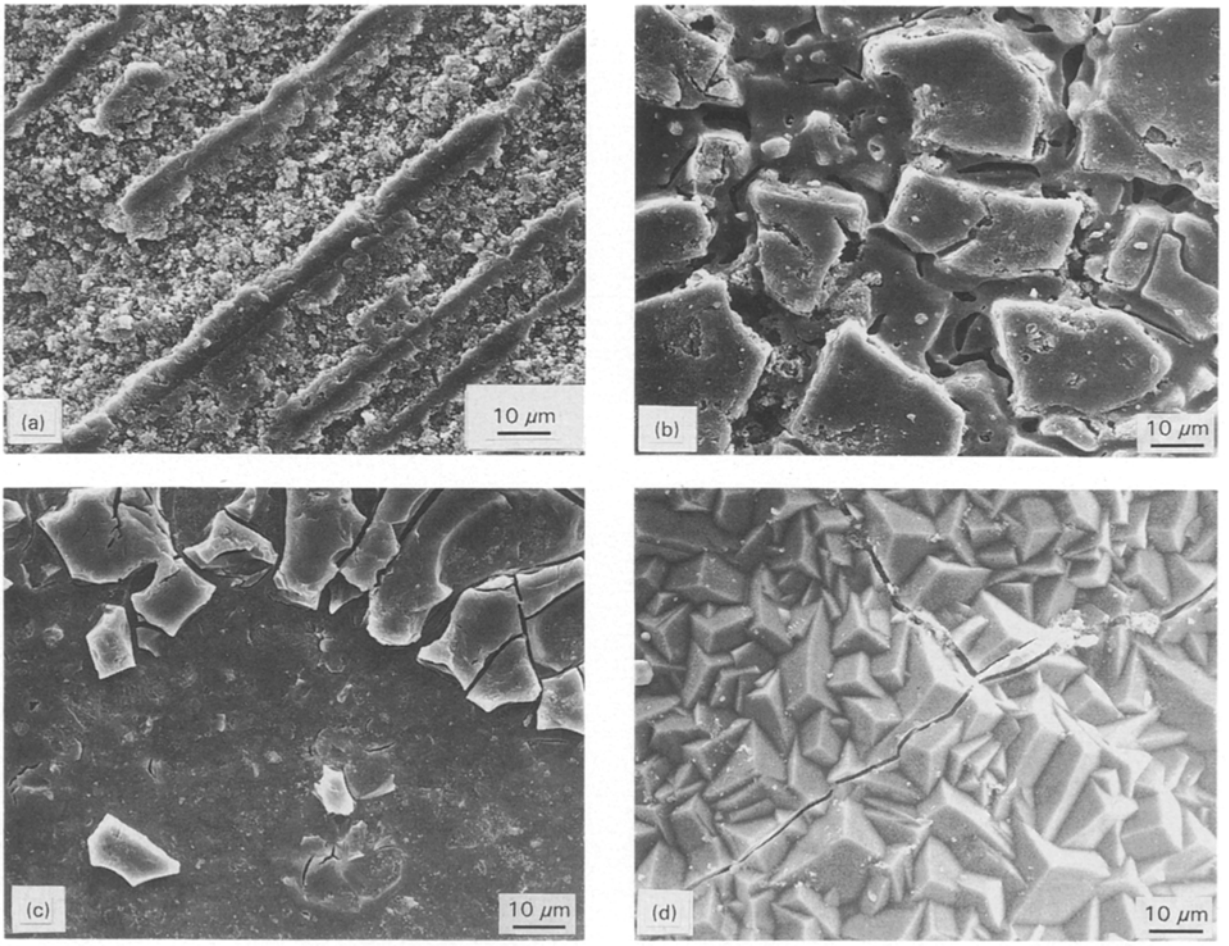

Figure 5 Surface morphology of monolithic RBSN after oxidation in 100 cc min^{-1} dry flowing oxygen: (a) type U (uncoated, 1000 °C, 168 h), (b) type A (Si–N–C, 1000 °C, 200 h), (c) type B (Si–C–O, 1000 °C, 185 h), (d) type C (CVD Si_3N_4, 900 °C, 240 h).

TABLE I Average per cent weight gain for uncoated monolithic RBSN

Temperature (°C)	Initial weight (g)	Outer surface area (cm^2)	Δ mass/initial mass 100 h (%)
900	1.09	5.23	3.5
	1.29	6.35	3.1
1000	1.34	6.56	12.3
	1.38	6.46	4.3
	1.28	6.52	6.5

which point surface oxidation became dominant. Bhatt [3] previously observed similar behaviour for this material at 1000 °C. A plot of $(\Delta W/A)^2$ versus time at both 900 and 1000 °C yields essentially straight lines. This signifies that parabolic oxidation of the internal porosity dominated and continued at the same rate throughout the experiment.

All of the coatings studied in this paper impede oxidation of monolithic RBSN. The primary reason is that internal porosity is sealed off by the surface coatings. However, the oxidation of the coating itself then comes into play. Type A materials (Si–N–C coating) exhibited linear weight gain at 900 and 1000 °C. This indicates that the formation of oxide on the coating was not limited by oxygen diffusion in the growing oxide. Linear kinetics are undesirable in engine applications where high flow rates are encountered. The coating was much more cracked than before exposure (Fig. 5b).

At 900 °C, Type B samples (Si–C–O coating) exhibited complex kinetics. An instantaneous weight loss was observed, possibly due to oxidation of carbon. After approximately 100 h, weight change was negligible. At 1000 °C, the Type B samples exhibited an initial rapid weight loss followed by a very slight linear weight loss, again likely due to the continued oxidation of free carbon in the coating. Spallation of the topmost coating layer occurred, though morphology of lower layers was not affected by the exposure (Fig. 5c).

Oxidation kinetics of Type C material at 900 °C were parabolic, though the rate constant was orders of magnitude higher than literature values for pure CVD Si_3N_4. Surface cracks were observed that penetrated the coating and continued into the RBSN. Such flaws would be deleterious to oxidation resistance as well as material strength. Calculated oxidation rate constants for all materials are summarized in Table II.

3.2. SiC–RBSN composite

As noted above, the Type B (Si–C–O) coating improved the oxidation resistance of uncoated, monolithic RBSN. The effect of this coating on the oxidation of SiC–RBSN was investigated. Weight change at

TABLE II Rate constants

Temperature (°C)	Material	k_p ($mg^2\ cm^{-4}\ h$)	k_l ($mg\ cm^{-2}\ h$)
900[a]	Uncoated	0.37	–
	Type A	–	0.014
	Type C	0.07	–
1000	Uncoated	3.51	–
	Type A	–	0.026
	Type B	–	– 0.004

[a] Type B kinetics at 900 °C are too complex to be characterized as linear or parabolic.

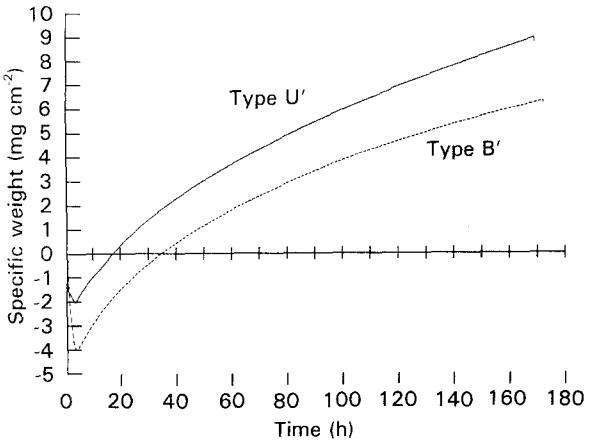

Figure 6 Oxidation kinetics of SiC–RBSN at 1000 °C in 100 cc min^{-1} dry flowing oxygen: type U′ (uncoated), type B′ (Si–C–O).

1000 °C of a single specimen of coated (Type B′) composite was measured and compared to uncoated (Type U′) SiC–RBSN. The results are shown in Fig. 6. The weight loss of the uncoated material at the beginning of the exposure is due to "tunnelling" oxidation of the carbon coating and core at the exposed fibre ends, and to a lesser degree internal oxidation of the fibre coatings. After approximately 5 h, weight gain due to silica formation dominates the reaction.

The kinetic trace of the coated Type B′ composite exhibits considerable similarity to that of the uncoated material. A weight loss is again measured in the first 5 h, though to a greater extent. This signifies no protection at short times due to the coating. The parabolic portion of the curve (time > 5 h) exactly duplicates that of uncoated SiC–RBSN.

Surface morphology of the coated material before and after oxidation is shown in Fig. 7. As-coated Type B′ SiC–RBSN is similar in appearance to as-coated Type B monolithic RBSN. However, after oxidation a number of perturbations are observed. Areas of bloating and cracking of the coating are observed, likely caused by escape of CO due to fibre coating oxidation (Fig. 7b). More disturbing is the appearance of matrix cracks that run parallel to the fibres. The exact cause of these cracks is unknown. One possible explanation is that thermal expansion differences between the composite and the coating cause high tensile stresses at the surface. Other causes could be carbothermal reactions or a large pressure buildup of CO in the

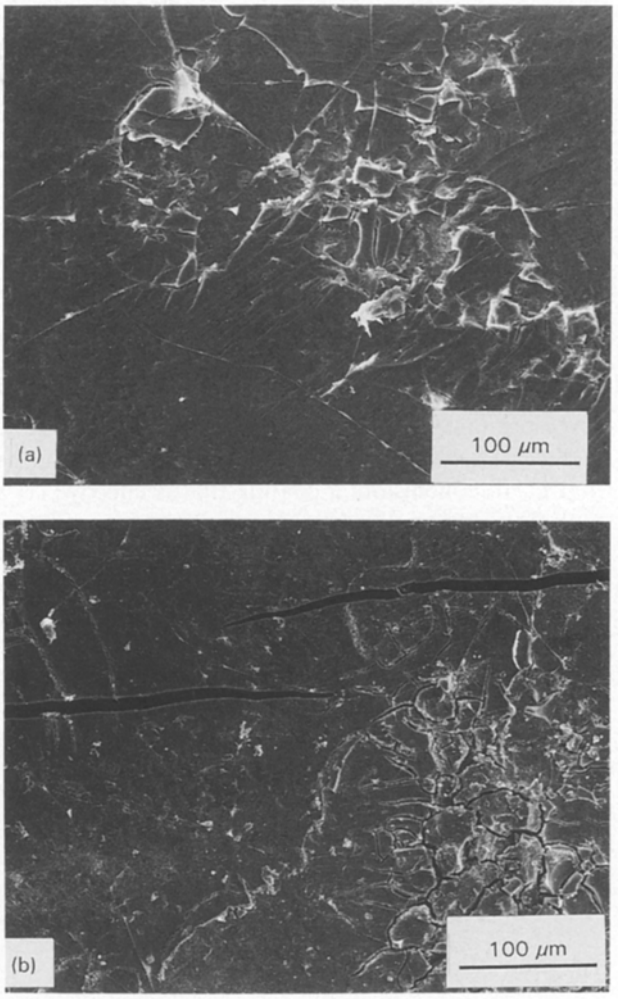

Figure 7 Surface morphology of type B′ coated SiC–RBSN: (a) prior to oxidation, (b) after 170 h oxidation in 100 cc min^{-1} dry flowing oxygen at 1000 °C; 10 μm wide cracks run parallel to SCS-6 fibres.

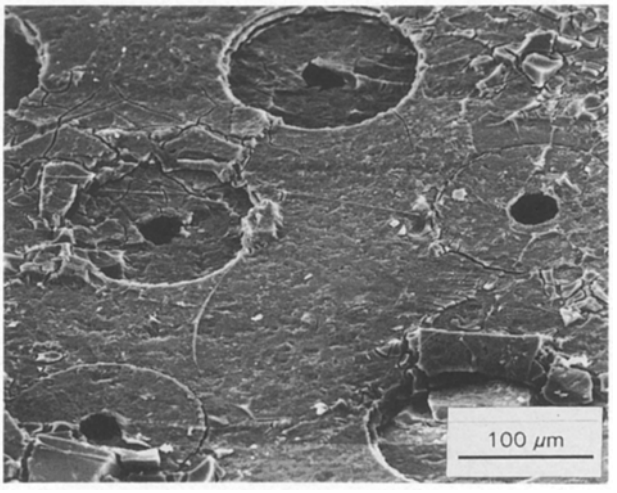

Figure 8 Surface morphology of type B′ coated SiC–RBSN at end of composite after 170 h oxidation in 100 cc min^{-1} dry flowing oxygen at 1000 °C.

composite due to fibre coating oxidation. These cracks open the interior of the composite to oxidation, as well as act as major flaws. Such cracks are not seen in uncoated, oxidized composites. A view of the ends of the coated composite (Fig. 8) after exposure shows reaction at the fibre–matrix interface, as well as oxidation of the fibre core. The Si–C–O coating therefore

does not provide adequate protection of the SiC–RBSN material, particularly over the top of the fibre ends.

4. Conclusions

It has been shown that the oxidation behaviour of porous, monolithic RBSN at 900 and 1000 °C in flowing oxygen can be improved via a number of surface coatings. At present, an amorphous Si–C–O material shows the greatest promise of the materials studied. However, when applied to SiC–RBSN composites, this coating provides inadequate protection to oxidation. Ruptures occur, particularly over fibre ends, and deleterious longitudinal cracks form in the matrix. In conclusion, a coating that is effective on a monolithic matrix material is not necessarily effective on fibre–reinforced composites utilizing the same matrix. Further coating systems must therefore be investigated to protect SiC–RBSN from oxidation.

Acknowledgements

The author would like to thank Dr E. J. Opila and Dr R. T. Bhatt for helpful discussions.

References

1. R. T. BHATT, US Patent No. 4689188 (1987).
2. R. W. DAVIDGE, A. G. EVANS, D. GILLING and P. R. WILYMAN, in "Special Ceramics", Vol. 5, edited by P. Popper (British Ceramic Research Association, Manchester, 1972) p. 329.
3. R. T. BHATT, *J. Amer. Ceram. Soc.* **75** (1992) 406.
4. S. P. HOWLETT, R. MORRELL and R. TAYLOR, *Brit. Ceram. Soc. Proc.* **37** (1986) 81.
5. L. J. LINDBERG, D. W. RICHERSON, W. D. CARRUTHERS and H. M. GERSCH, *Bull. Amer. Ceram. Soc.* **61** (1982) 574.
6. S. C. SINGHAL, in "Nitrogen Ceramics", edited by F. L. Riley (Noordhoff, Leyden, 1977) p. 607.
7. F. PORZ and F. THUMMLER, *J. Mater. Sci.* **19** (1984) 1283.
8. A. G. EVANS and R. W. DAVIDGE, *ibid.* **5** (1970) 413.
9. W. ZDANIEWSKI, D. P. H. HASSELMAN, H. KNOCH and J. HEINRICH, *Bull. Amer. Ceram. Soc.* **58** (1979) 539.
10. O. J. GREGORY and M. H. RICHMAN, *J. Amer. Ceram. Soc.* **67** (1984) 335.
11. A. P. M. ADRIAANSEN and H. GOOIJER, *Euro. Ceram.* **3** (1989) 569.
12. J. DESMAISON, N. ROELS and P. BELAIR, *Mater. Sci. Engng* **A121** (1989) 441.
13. J. SCHLICHTING and S. NEUMANN, *J. Non-Cryst. Solids* **48** (1982) 185.

Received 25 May 1993
and accepted 10 May 1994